NK cells control breast cancer and related cancer stem cell hematological spread

Tallerico, Rossana; Conti, Laura; Lanzardo, Stefania; Sottile, Rosa; Garofalo, Cinzia; Wagner, Arnika K.; Johansson, Maria H.; Cristiani, Costanza Maria; Kärre, Klas; Carbone, Ennio; Cavallo, Federica. NK cells control breast cancer and related cancer stem cell hematological spread. ONCOIMMUNOLOGY. 6 (3) pp: e1284718-e1284728. DOI: 10.1080/2162402X.2017.1284718

OncoImmunology

ISSN: (Print) 2162-402X (Online) Journal homepage: http://www.tandfonline.com/loi/koni20

NK cells control breast cancer and related cancer stem cell hematological spread

Rossana Tallerico, Laura Conti, Stefania Lanzardo, Rosa Sottile, Cinzia Garofalo, Arnika K. Wagner, Maria H. Johansson, Costanza Maria Cristiani, Klas Kärre, Ennio Carbone & Federica Cavallo

To cite this article: Rossana Tallerico, Laura Conti, Stefania Lanzardo, Rosa Sottile, Cinzia Garofalo, Arnika K. Wagner, Maria H. Johansson, Costanza Maria Cristiani, Klas Kärre, Ennio Carbone & Federica Cavallo (2017): NK cells control breast cancer and related cancer stem cell hematological spread, OncoImmunology, DOI: 10.1080/2162402X.2017.1284718

To link to this article: http://dx.doi.org/10.1080/2162402X.2017.1284718

Brief Report

NK cells control breast cancer and related cancer stem cell hematological spread.

Rossana Tallerico[1,*], Laura Conti[2,*], Stefania Lanzardo[2,*], Rosa Sottile[1,3], Cinzia Garofalo[1], Arnika K. Wagner[3], Maria H. Johansson[3], Costanza Maria Cristiani[1], Klas Kärre[3], Ennio Carbone[1,3,*] and Federica Cavallo[2,*]

[1]Tumor Immunology and Immunopathology Laboratory, Department of Experimental and Clinical Medicine, University Magna Graecia of Catanzaro, Catanzaro, Italy

[2]Department of Molecular Biotechnology and Health Sciences, Molecular Biotechnology Center, University of Turin, Turin, Italy

[3]Department of Microbiology, Cell and Tumor biology (MTC), Karolinska Institutet, Stockholm, Sweden

[*]These authors contributed equally.

Corresponding authors: Rossana Tallerico

Tumor Immunology and Immunopathology Laboratory, Department of Experimental and Clinical Medicine, University Magna Graecia of Catanzaro,Viale Europa – Loc. Germaneto, 88100, Catanzaro, Italy, rossana.tallerico@gmail.com

Stefania Lanzardo. Molecular Biotechnology Center, Via Nizza 52, 10126, Torino, Italy, stefania.lanzardo@unito.it

Abstract

The growth and recurrence of a number of cancers is driven by a scarce population of cancer stem cells (CSCs), which are resistant to most current therapies. It has been shown previously that Natural Killer (NK) cells recognize human glioma, melanoma, colon and prostate CSCs *in vitro*. We herein show that human and mouse breast CSCs are also susceptible to NK cytotoxic activity *in*

vitro. Moreover, CSC induced autologous NK cell activation and expansion *in vivo,* which correlate with the inhibition of CSC metastatic spread. These data suggest that NK cells control CSC metastatic spread *in vivo* and that their use in breast cancer therapy may well be fruitful.

Keywords

NK cells, CSCs, tumorspheres, metastasization, immunotherapy, breast cancer

Introduction

The last century has seen a great deal of speculation as to the processes underlying the etiology of cancer and several theories have been put forward.[1, 2] The fact that any cell exposed to genotoxic stress is able to generate a tumor has received general agreement.[3] Meanwhile, stochastic influences have more recently been found to be major contributors to cancer development. They are nowadays often considered more important than either hereditary or external environmental factors. Most genomic changes occur simply by chance during DNA replication. Considering the number of mutations needed for malignant transformation, it appears highly plausible that these can only accumulate in long-lived cells, i.e. stem cells.[4]

Cancer stem cells (CSCs) have recently been proposed as a key compartment of the tumor population.[5, 6] Similarly to normal stem cells, CSCs are a slowly proliferating population which is able to self-renew and give rise to more differentiated cells that compose the bulk of a tumor.[7] CSCs have also been hypothesized to be a crucial factor in tumor recurrence, due to their intrinsic resistance to drugs and irradiation which often enables them to survive traditional therapies. Moreover, they have been demonstrated to be responsible for the hematological metastatic spread of solid tumors.[8]

Therefore, the question of whether cells of the CSC phenotype and tumorigenic potential are common or rare within human cancers has fundamental implications for therapy.[9] If tumorigenic cells are a small minority population, as suggested by the cancer stem cell theory,[10, 11] improved anti-cancer therapies may be identified based on their ability to kill CSCs, rather than the bulk population of non-tumorigenic cancer cells.[12, 13]

It is furthermore wise to explore whether effector immune cytotoxic cells (NK cells, CD8 T cells and γδ T cells) can be used to eliminate the tumor stem cell compartment in order to limit the CSC contribution to sustaining tumor progression. The low levels of MHC class I expression reported in CSCs hints at the low efficiency of CSC targeting by CD8 T lymphocytes.[14, 15] However, the expression of ligands for NK activating receptors (NKG2D, NCR and DNAM-1)[15-17] points to NK

cells and other innate immunity effector cells being able to recognize and eliminate CSCs. Indeed, recent data have demonstrated that human γδ T cells can target CSCs *in vitro*.[18]

Human and murine NK cells are members of group 1 of Innate Lymphoid Cells.[19] Their activation is regulated by activating receptors which recognize stress inducible ligands (NKG2D, DNAM-I) and the IgG Fc domain (CD16).[20] NK cell tolerance is maintained by the engagement of inhibitory receptors which principally recognize MHC class I molecules (KIRs in humans, Ly49 receptors in mice).[21]

Previous data have shown that NK cells selectively kill CSCs derived from human colon carcinoma,[15] melanoma[16] and glioblastoma,[17] in mainly *in vitro* experiments. We herein describe *in vitro* and *in vivo* experiments which validate the NK cell targeting of breast tumor-derived CSCs using CSC-enriched tumorsphers[22] derived from an ErbB-2$^+$ murine breast cancer tumor cell line (TUBO),[23] and murine and human triple negative breast cancer (TNBC) cell lines.

Results and Discussion

Tumorspheres derived from the murine ErbB2$^+$ tumor cell line, TUBO, were used to evaluate whether NK cells are able to recognize breast cancer derived CSCs. CSC enrichment in tumorspheres was confirmed via the increased percentage of cells that were positive for aldehyde dehydrogenase (ALDH) activity and for stem cell markers, Sca-1 and Thy1.1, as compared to TUBO parental cells (Fig. 1A and B, respectively), as has already been observed in previous reports.[22, 24]Moreover, tumorspheres showed increased *in vitro* self-renewal, with respect to TUBO cells in our own experiments. This is demonstrated by the higher number of cell clones generated by tumorspheres in a limiting dilution assay (Fig. 1C), confirming that they possess higher enrichment in CSCs than TUBO cells. Injecting TUBO and tumorspheres s.c. into BALB/c mice led to the observation that $1x10^3$ tumorsphere-derived cells gave rise to a fast growing palpable tumor in 100% mice, while the same number of TUBO cells induced a palpable tumor in only 66.7% of mice and did so with very slow kinetics (Fig. 1D, E). Moreover, mice injected with TUBO cells

exhibited significantly longer median survival times than mice injected with tumorsphere-derived cells (Fig. 1F).

TUBO and tumorsphere susceptibility to autologous and allogeneic NK cell recognition was initially analyzed *in vitro* (Fig. 2). Highly purified autologous and allogeneic NK cells were obtained from the spleens of BALB/c and C57/BL6 mice, respectively. In both experimental settings, tumorspheres were recognized and killed with higher efficiency than TUBO cells (Fig. 2A, B). These observations are in agreement with those previously reported in other human solid tumor experimental systems.[15-17, 25] In Figure 2, NK cells were activated with IL2 *in vitro*, whereas autologous and allogeneic NK cells were used as effectors without any activation in Table 1. Surprisingly, tumorspheres were selectively killed even when freshly explanted NK cells were used as effectors. It should be emphasized that the recognition of tumorspheres by non-activated murine NK cells is one of the few biological conditions in which non-activated NK cells can target tumor cells.

In order to understand the molecular mechanisms that regulate selective NK mediated CSC elimination, we investigated the surface expression of inhibitory (H2-K^d, H2-D^d) and activating ligands (NKp46L, RAE, H60, PVR, Nectin-2) on tumorspheres and TUBO cells. Reduced H2-K^d frequency and expression were observed together with an upregulation in PVR on the tumorsphere cell membrane (Fig. 3A, B). This latter finding confirms previous observations describing the crucial role that DNAM-1 ligands play in the NK recognition of CSCs.[26] H2-D^d and the activating ligands for NKG2D and NCRs were expressed in similar amounts on both tumor cell types (Fig. S1A, B). The expression of NK activating and inhibitory ligands was evaluated using FACS in order to explore whether tumors and lung metastases induced in BALB/c mice via the s.c. or i.v. injection of either TUBO or tumorspheres maintain the differences in their expression rates. Interestingly, we have previously reported that tumorspheres maintain a prevalent CSC phenotype after *in vivo* injection[27]. As reported in Fig. 4, a lower frequency of H2-K^d and a higher frequency and expression of activating ligands, RAE, H60, PVR and Nectin-2, were observed in both the

tumorsphere generated tumors and metastases than in their TUBO generated analogues. Therefore, the immune phenotype that emerges from our data, which is characterized by a reduced number of MHC-I^+ tumorspheres expressing higher levels of DNAM-1 activating ligands (PVR and Nectin-2), nicely correlates with the higher susceptibility of tumorspheres to NK cell recognition. However, we cannot exclude that in vivo other activating NK receptors besides DNAM-1 may play a role in the tumorsphere higher NK cells susceptibility, as suggested by the increased expression of RAE and H60 by tumorspheres (Fig. 4A).

The possible role of DNAM-1 receptors in driving tumorsphere recognition by NK cells was partially explored in functional experiments using DNAM-1 KO mice. Indeed, the data obtained suggests that NK cells derived from DNAM-1 KO mice display lower tumorsphere cytotoxicity recognition efficiency (Fig. S2A).

It is worth noting that the *in vitro* NK cell recognition of breast cancer derived CSCs is not restricted to the TUBO model, as was also observed in CSCs derived from murine (4T1) and human (HCC-1806 and MDA-MB-231) TNBC cell lines. In fact, MHC-I expression decreased in tumorspheres derived from all of these cell lines (Fig. S3A and Fig. 5A, B). Moreover, an analysis of NK activating ligands, RAE, H60, PVR and Nectin-2, showed enhanced expression in 4T1-derived tumorspheres over 4T1 cells (Fig. S3A). As reported in Figure 5C-F, allogeneic human NK cells, which had been isolated from healthy donors' PBMC, recognized and killed tumorspheres generated from both HCC-1806 and MDA-MB-231 cells with higher efficiency than those generated by the two parental cell lines. Similar results were obtained on tumorspheres derived from 4T1 cells, which displayed higher susceptibility to autologous and allogeneic NK cell recognition than 4T1 cells (Fig. S3B).

In order to evaluate any potential role that NK cells may play in controlling the hematological metastasization of TUBO cells and their derived tumorspheres in autologous conditions, BALB/c mice were divided into two different groups that received either TUBO or tumorsphere-derived cells i.v.. Each group was further divided into three subgroups in which the NK cell compartment

was manipulated by either depleting NK cells with a neutralizing antibody (TMβ1)[28, 29] or by activating NK cell cytotoxicity with an interferon type I inducer (tilorone).[30] The third group of mice was treated with PBS as a control. Twenty-one days after cell injection, mice were sacrificed and lung metastases were counted and analyzed for size after H&E staining. As reported in Figure 6, TUBO cell injection gave rise to a higher number of lung metastases in the control groups than in mice injected with tumorspheres (Fig. 6A, B). Moreover, the metastasis occupied lung surface was larger in mice injected with TUBO than in mice injected with tumorspheres (Fig. 6 D-F), suggesting that the NK cell-mediated elimination of CSCs is more pronounced here than in TUBO cells. NK cell depletion led to an increased number of lung metastases in TUBO, as well as in tumorsphere, injected mice, while NK cell activation by tilorone furnished a beneficial effect by limiting the lung metastatic spread in both experimental groups (Fig. 6A, B). It can therefore be stated that NK cells control the spread of both cell types *in vivo*. However, an analysis of the relative NK cell capability to control the metastatic spread of the bulk tumor population and/or CSCs revealed that NK manipulation had a stronger effect on tumorsphere metastatic spread (Fig. 6C), confirming the importance of NK cells in killing CSCs. This is confirmed by the observation that neither TMβ1 nor tilorone exert any effect on the amount of lung surface occupied by TUBO metastases, while they both significantly modify the area occupied by tumorsphere metastases (Fig. 6D-F). It should be noted that tumorspheres injected s.c. showed higher tumorigenicity than injected TUBO cells. We can speculate that this difference may reflect the different activation mechanisms that NK cells depend on in the blood and lungs, as reported in BL6 mice for NK cell *in vivo* control of the melanoma spread in the peritoneum and lung.[31]

To understand whether the contrasting findings observed after the intravenous infusion of tumor cells were actually due to differences in NK cells, we analysed their expansion and activation in BALB/c mice injected s.c. and i.v. with either TUBO or tumorspheres, while a further group was left untreated. Mice injected i.v. were sacrificed 21 days after challenge while those injected s.c. were sacrificed when the tumor reached 5 mm in mean diameter. Blood, lung and tumor NK cell

frequencies and activation markers were analyzed. In the blood, $CD49b^+$ NK cell frequency increased in the group that received tumorspheres i.v., as compared to all other groups (Fig. 7). Moreover, a higher frequency of circulating $CD69^+$ NK cells was found in mice injected with tumorspheres, whether i.v. or s.c., as compared to other groups (Fig. 7). A detailed analysis of the different NK cell compartments in the blood of mice injected i.v. with either TUBO or tumorspheres was performed and is reported in Figure S4. It is worth noting that tumorsphere injection did not induce the expansion of T cell subsets (Fig. S5). The i.v. challenge with breast cancer derived CSCs thus selectively induced the expansion of the activated NK cell compartment, as previously reported in *in vitro* co-culture experiments conducted using autologous NK cells and human colon adenocarcinoma derived CSCs.[15] However, the lack of $Ly49H^+$ in BALB/c mice prevented us from better defining NK cell expansion, i.e. the NK cell memory subset associated with MCMV infected mice.[32]

An analysis of the NK cell population infiltrating lung metastases and s.c. tumors revealed that the highest frequency of NK cells was observed in the lungs of mice injected i.v. with tumorspheres (Fig. 8 C, E). Interestingly, the NK population was more abundant in lung metastases than in s.c. tumors (Fig. 8 A-E) in both mice injected with TUBO and tumorspheres. The evaluation of NK activation displayed a higher percentage of $CD69^+$ cells among the NK cells present in both lung metastases and the tumors of mice injected with tumorspheres than in TUBO-injected mice (Fig. 8 A-E).

In conclusion, our data show that *in vivo* murine breast cancer tumorspheres induce NK cell compartment expansion and promote their activation. Moreover, the *in vivo* manipulation of NK cell response affects the capability of tumorspheres to undergo lung metastatic spread. It has recently been reported that human $ALDH^+$ CSCs, derived from human breast cancer, escape NK recognition by down regulating NKG2D ligands, thanks to the expression of miR20a.[33] Our data in mice expand this finding and indicate that not all breast cancer derived CSCs are resistant to NK cell cytotoxic attack.

Our data corroborate previous *in vitro* observations obtained using human solid tumors and related CSCs,[12-14] and strongly suggest that NK cells should be considered a potential useful tool in therapy protocols that aim to target the tumor CSC compartment.

Material and Methods

Cell lines

ErbB2$^+$ murine breast tumor parental TUBO cells were cultured in DMEM 20% FBS.[34] Murine (4T1) and human (HCC-1806 and MDA-MB-231) breast cancer parental cells were purchased from ATCC (LCG Standards) and cultured in RPMI plus 10% FBS or DMEM 10% FBS, respectively. Tumorspheres were generated by culturing TUBO, 4T1, MDA-MB-231 and HCC-1806 cells in ultra-low attachment flasks (Sigma-Aldrich) in DMEM-F12 supplemented with 0,4% bovine serum albumin (Sigma-Aldrich), 20 ng/ml basic Fibroblast Growth Factor (bFGF, Peprotech), 20 ng/ml Epidermal Growth Factor (EGF, Sigma-Aldrich) and 5 μg/ml insulin (Sigma-Aldrich). They were propagated *in vitro* up to the third passage (P3, hereafter referred as tumorspheres), as previously described.[24]

In Vivo Treatments

BALB/c and C57/BL6 mice were bought from Charles River Laboratories, maintained at the Molecular Biotechnology Center, University of Turin and treated in accordance with University Ethical Committee and European guidelines under Directive 2010/63.

Primary s.c. tumors were induced by injecting the flank of female BALB/c mice with either $1x10^4$ TUBO or tumorsphere-derived cells (n=6 for both conditions). Tumor growth was monitored weekly by caliper and reported as the mean of two perpendicular diameters (mm). Mice were sacrificed for ethical reasons when tumors reached 10 mm mean diameter.[35, 36] Lung metastases were induced by injecting BALB/c mice i.v. with either $5x10^4$ TUBO or tumorsphere-derived cells. Each group was further divided into three subgroups (n=5 mice each) in which mice were either treated per os with tilorone (200 μg, Sigma-Aldrich) the day before cell challenge and then every 3 days, treated i.v. with an anti-mouse-TMβ1 monoclonal antibody (200 μg, Mabtech) the day before

cell injection and then every 7 days, or finally treated with PBS (as control). Twenty-one days after cell injection, blood was collected and mice were sacrificed in order to analyze lung metastasis formation and immune infiltrate both by FACS and histological analysis. Lungs were removed, fixed in 4% formaldehyde solution, cut into small pieces, paraffin-embedded, sectioned and haematoxylin and eosin (H&E) stained.[37] Micrometastases were counted on a Nikon SMZ1000 stereomicroscope (Amsterdam, Netherlands), their dimensions measured using ImageJ software and reported as the ratio between the area occupied by metastases and total lung area, as previously described.[19,38]

DNAM-1 KO mice[39] were kindly provided by M Colonna Washington University Medical School, St Louis, MO. These mice and C57/BL6 mice were housed under specific pathogen–free conditions at the Department of Microbiology, Tumor and Cell Biology, Karolinska Institute. Experiments were performed according to governmental and institutional guidelines and regulations were approved by the local ethical committee (North Stockholm District Court).

Tumor and lung dissociation for FACS analysis

For the phenotypic analysis, fresh primary tumor specimens of 5 mm mean diameter and lungs from BALB/c mice injected either s.c. or i.v. with TUBO or tumorspheres were finely minced with scissors and then digested by incubation with 1 mg/mL collagenase IV (Sigma Aldrich) in RPMI-1640 (Life Technologies) at 37°C for 1 h in an orbital shaker. After washing in PBS supplemented with 2% fetal calf serum (GIBCO), the cell suspension was incubated in erylise buffer (155 mM NH_4Cl, 15.8 mM Na_2CO_3, 1 mM EDTA, pH 7.3) for 10 min at RT. After washing in RPMI-1640 supplemented with 10% FBS, the cell suspension was passed through a 70-µm pore cell strainer, centrifuged at 1400 rpm for 10 min and re-suspended in erylise buffer. Cells were collected, washed, re-suspended in PBS, treated with Fc-receptor blocker and stained for FACS analysis.[40, 41]

Flow cytometry

Cells derived from tumors and metastases, parental cells and tumorspheres harvested after 5 days of culture were washed in PBS supplemented with 0.2% BSA and 0.01% sodium azide (Sigma-Aldrich) and stained as previously described,[42, 43] with the following antibodies: Alexa Fluor647-conjugated anti-Stem Cell Antigen (Sca)-1, allophycocyanin (APC)/Alexa Fluor780-conjugated anti-Thy1.1, FITC HLA-I clone w6/32 (BioLegend), FITC-conjugated anti-H2-K^d, FITC-conjugated anti-H2-D^d (Becton Dickinson) PE-conjugated H60 (R&D), pan RAE1-FITC (R&D), Nectin-2-APC (R&D) or with mouse NCR1-Ig (10 μg/ml) followed by Alexa Fluor 647 donkey anti-human Ig, kindly provided by Prof. F. Colucci, Cambridge University, UK. The ALDEFLUOR assay was performed to evaluate aldehyde dehydrogenase (ALDH) activity according to manufacturer's instructions (Stem Cell Technologies, Vancouver, Canada). Cells were analyzed on a CyAnADP Flow Cytometer, using Summit 4.3 software (Beckman Coulter). Data were evaluated using FlowJo (Mac-Version 9.3.1; Treestar US, Ashland, OR) or Summit 4.3 software.

Clonal formation assay

TUBO cells and tumorspheres were plated at 1 cell/well in 96-well plates or in 96-well ultra-low attachment plates, containing 150 μl of epithelial or tumorsphere medium, respectively. The number of TUBO or tumorsphere clones generated after 7 days of culture was evaluated and reported as number of clones generated for every 100 single cells seeded.

NK cell isolation

To isolate NK cells, spleens were collected from 8 week-old female BALB/c and C57/BL6 mice (either treated 1 day before sacrifice with 200 μg tilorone per os, Sigma-Aldrich, or left untreated), and mashed in order to obtain splenocytes. For experiments with DNAM-1-KO and C57/BL6 mice, animals were treated i.p. with 100μg poly-I:C two days prior to NK cell isolation. Enriched NK cells were isolated from the separated splenocytes using murine NK Cell Isolation Kit II (Miltenyi Biotec) according to manufacturer's instructions. NK cells were cultured overnight in RPMI 10% FBS and 1% Penicillin/Streptomycin, either with or without 200 U/ml IL-2 (Peprotech). For human NK cells, blood was obtained from healthy donors and peripheral blood lymphocytes were isolated

by Biocoll separating solution (Biochrom AG) density gradient centrifugation. Enriched NK cells were isolated from the separated PBMCs using the NK cell isolation kit (Miltenyi Biotec) according to manufacturer's instructions. NK cells were cultured overnight in RPMI 10% FBS and 1% Penicillin/Streptomycin. The purity of isolated NK cells was > 95%, as assayed by flow cytometry.

Cytotoxicity assays

Cytotoxic assays were performed using fluorescent 5,6-carboxy-fluorescein-diacetate (CFDA) according to a protocol described elsewhere.[44] Briefly, target cells were labeled with CFDA-mixed isomers (Invitrogen) and then with purified autologous and allogeneic NK effector cells at different Effector:Target (E:T) ratios. The incubation was performed in 96-well U-bottom plates at 37° C in a humidified 5% CO_2 incubator for 3 h. The specific lysis of target cells was analyzed by flow cytometry (FACS CantoII, BD Pharmingen) and calculated as follows: % of specific lysis = (CT-TE)/CT x 100, where CT indicates the mean number of fluorescent target cells in control tubes and TE indicates the mean number of fluorescent cells in target plus effector tubes. Data were evaluated using FlowJo (Mac-Version 9.3.1; Treestar US, Ashland, OR).

NK cell immunophenotype

Lymphocytes from the blood of mice were washed twice in PBS and then incubated with erylise buffer (155mM NH_4Cl, 15.8mM Na_2CO_3, 1mM EDTA, pH 7.3) for 10 minutes at room temperature, washed in PBS and incubated with a purified anti-mouse *CD16/CD32 (BD Pharmingen)* for 10 minutes at room temperature. These cells and cells obtained from tumors and metastases were washed with PBS and then labeled for 30 minutes at 4° C with the following antibodies: FITC-conjugated anti-CD49b/DX5, APC/Cy7-conjugated anti-CD3, PE-conjugated anti-DNAM-I, APC-conjugated anti-NKp46, PerCp/Cy5.5-conjugated anti-CD69, Pacific Blue-conjugated anti-LY49a (all from BioLegend), PE/Cy7-conjugated anti-NKG2D (eBioscience), PE-conjugated anti-5E6 (BD). Cells were analyzed on a CyAnADP Flow Cytometer, using Summit 4.3 software (Beckman Coulter). Data were evaluated using either FlowJo (Mac-Version 9.3.1; Treestar US, Ashland, OR) or Summit 4.3 software.

Statistical analysis

Statistical analysis was performed using GraphPad Prism 5.0 Software. Either the unpaired Student's t test and ANOVA Analysis or the Mann-Whitney test were used for non-parametric distributions to determine significance. Differences in tumor incidence and survival were analyzed using Mantel-Cox log-rank tests. A p value ≤ 0.05 was considered significant. * $p \leq 0.05$; ** $p \leq 0.01$; ***$p \leq 0.001$.

References

1. Bignold LP, Coghlan BL, Jersmann HP. Hansemann, Boveri, chromosomes and the gametogenesis-related theories of tumours. Cell Biol Int 2006; 30:640-4.

2. Sell S. Stem cell origin of cancer and differentiation therapy. Crit Rev Oncol Hematol 2004; 51:1-28.

3. Knudson AG, Jr., Strong LC, Anderson DE. Heredity and cancer in man. Prog Med Genet 1973; 9:113-58.

4. Tomasetti C, Vogelstein B. Cancer risk: role of environment-response. Science 2015; 347:729-31.

5. Fornari C, Beccuti M, Lanzardo S, Conti L, Balbo G, Cavallo F, et al. A mathematical-biological joint effort to investigate the tumor-initiating ability of Cancer Stem Cells. PLoS One 2014; 9:e106193.

6. Cordero F, Beccuti M, Fornari C, Lanzardo S, Conti L, Cavallo F, et al. Multi-level model for the investigation of oncoantigen-driven vaccination effect. BMC Bioinformatics 2013; 14 Suppl 6:S11.

7. Conti L, Ruiu R, Barutello G, Macagno M, Bandini S, Cavallo F, et al. Microenvironment, oncoantigens, and antitumor vaccination: lessons learned from BALB-neuT mice. Biomed Res Int 2014; 2014:534969.

8. Nicolini A, Ferrari P, Fini M, Borsari V, Fallahi P, Antonelli A, et al. Stem cells: their role in breast cancer development and resistance to treatment. Curr Pharm Biotechnol 2011; 12:196-205.

9. Quintana E, Shackleton M, Sabel MS, Fullen DR, Johnson TM, Morrison SJ. Efficient tumour formation by single human melanoma cells. Nature 2008; 456:593-8.

10. Reya T, Morrison SJ, Clarke MF, Weissman IL. Stem cells, cancer, and cancer stem cells. Nature 2001; 414:105-11.

11. Lobo NA, Shimono Y, Qian D, Clarke MF. The biology of cancer stem cells. Annu Rev Cell Dev Biol 2007; 23:675-99.

12. Pardal R, Clarke MF, Morrison SJ. Applying the principles of stem-cell biology to cancer. Nat Rev Cancer 2003; 3:895-902.

13. Wang JC, Dick JE. Cancer stem cells: lessons from leukemia. Trends Cell Biol 2005; 15:494-501.

14. Di Tomaso T, Mazzoleni S, Wang E, Sovena G, Clavenna D, Franzin A, et al. Immunobiological characterization of cancer stem cells isolated from glioblastoma patients. Clin Cancer Res 2010; 16:800-13.

15. Tallerico R, Todaro M, Di Franco S, Maccalli C, Garofalo C, Sottile R, et al. Human NK cells selective targeting of colon cancer-initiating cells: a role for natural cytotoxicity receptors and MHC class I molecules. J Immunol 2013; 190:2381-90.

16. Pietra G, Manzini C, Vitale M, Balsamo M, Ognio E, Boitano M, et al. Natural killer cells kill human melanoma cells with characteristics of cancer stem cells. Int Immunol 2009; 21:793-801.

17. Castriconi R, Daga A, Dondero A, Zona G, Poliani PL, Melotti A, et al. NK cells recognize and kill human glioblastoma cells with stem cell-like properties. J Immunol 2009; 182:3530-9.

18. Todaro M, D'Asaro M, Caccamo N, Iovino F, Francipane MG, Meraviglia S, et al. Efficient killing of human colon cancer stem cells by gammadelta T lymphocytes. J Immunol 2009; 182:7287-96.

19. Spits H, Artis D, Colonna M, Diefenbach A, Di Santo JP, Eberl G, et al. Innate lymphoid cells--a proposal for uniform nomenclature. Nat Rev Immunol 2013; 13:145-9.

20. Lanier LL. NK cell recognition. Annu Rev Immunol 2005; 23:225-74.

21. Orr MT, Lanier LL. Natural killer cell education and tolerance. Cell 2010; 142:847-56.

22. Conti L, Lanzardo S, Arigoni M, Antonazzo R, Radaelli E, Cantarella D, et al. The noninflammatory role of high mobility group box 1/Toll-like receptor 2 axis in the self-renewal of mammary cancer stem cells. FASEB J 2013; 27:4731-44.

23. Porzia A, Lanzardo S, Citti A, Cavallo F, Forni G, Santoni A, et al. Attenuation of PI3K/Akt-mediated tumorigenic signals through PTEN activation by DNA vaccine-induced anti-ErbB2 antibodies. J Immunol 2010; 184:4170-7.

24. Lanzardo S, Conti L, Rooke R, Ruiu R, Accart N, Bolli E, et al. Immunotargeting of Antigen xCT Attenuates Stem-like Cell Behavior and Metastatic Progression in Breast Cancer. Cancer Res 2016; 76:62-72.

25. Ames E, Canter RJ, Grossenbacher SK, Mac S, Chen M, Smith RC, et al. NK Cells Preferentially Target Tumor Cells with a Cancer Stem Cell Phenotype. J Immunol 2015; 195:4010-9.

26. Kruse V, Hamann C, Monecke S, Cyganek L, Elsner L, Hubscher D, et al. Human Induced Pluripotent Stem Cells Are Targets for Allogeneic and Autologous Natural Killer (NK) Cells and Killing Is Partly Mediated by the Activating NK Receptor DNAM-1. PLoS One 2015; 10:e0125544.

27. Conti L, Lanzardo S, Ruiu R, Cadenazzi M, Cavallo F, Aime S, et al. L-Ferritin targets breast cancer stem cells and delivers therapeutic and imaging agents. Oncotarget 2016.

28. Bosma GC, Custer RP, Bosma MJ. A severe combined immunodeficiency mutation in the mouse. Nature 1983; 301:527-30.

29. Mosier DE, Gulizia RJ, Baird SM, Wilson DB. Transfer of a functional human immune system to mice with severe combined immunodeficiency. Nature 1988; 335:256-9.

30. Brodin P, Lakshmikanth T, Mehr R, Johansson MH, Duru AD, Achour A, et al. Natural killer cell tolerance persists despite significant reduction of self MHC class I on normal target cells in mice. PLoS One 2010; 5.

31. Lakshmikanth T, Burke S, Ali TH, Kimpfler S, Ursini F, Ruggeri L, et al. NCRs and DNAM-1 mediate NK cell recognition and lysis of human and mouse melanoma cell lines in vitro and in vivo. J Clin Invest 2009; 119:1251-63.

32. Bezman NA, Kim CC, Sun JC, Min-Oo G, Hendricks DW, Kamimura Y, et al. Molecular definition of the identity and activation of natural killer cells. Nat Immunol 2012; 13:1000-9.

33. Wang B, Wang Q, Wang Z, Jiang J, Yu SC, Ping YF, et al. Metastatic consequences of immune escape from NK cell cytotoxicity by human breast cancer stem cells. Cancer Res 2014; 74:5746-57.

34. Geninatti Crich S, Cadenazzi M, Lanzardo S, Conti L, Ruiu R, Alberti D, et al. Targeting ferritin receptors for the selective delivery of imaging and therapeutic agents to breast cancer cells. Nanoscale 2015; 7:6527-33.

35. Rolla S, Marchini C, Malinarich S, Quaglino E, Lanzardo S, Montani M, et al. Protective immunity against neu-positive carcinomas elicited by electroporation of plasmids encoding decreasing fragments of rat neu extracellular domain. Hum Gene Ther 2008; 19:229-40.

36. Conti L, Lanzardo S, Iezzi M, Montone M, Bolli E, Brioschi C, et al. Optical imaging detection of microscopic mammary cancer in ErbB-2 transgenic mice through the DA364 probe binding alphav beta3 integrins. Contrast Media Mol Imaging 2013; 8:350-60.

37. Geninatti Crich S, Cutrin JC, Lanzardo S, Conti L, Kalman FK, Szabo I, et al. Mn-loaded apoferritin: a highly sensitive MRI imaging probe for the detection and characterization of hepatocarcinoma lesions in a transgenic mouse model. Contrast Media Mol Imaging 2012; 7:281-8.

38. Principe M, Ceruti P, Shih NY, Chattaragada MS, Rolla S, Conti L, et al. Targeting of surface alpha-enolase inhibits the invasiveness of pancreatic cancer cells. Oncotarget 2015; 6:11098-113.

39. Gilfillan S, Chan CJ, Cella M, Haynes NM, Rapaport AS, Boles KS, et al. DNAM-1 promotes activation of cytotoxic lymphocytes by nonprofessional antigen-presenting cells and tumors. J Exp Med 2008; 205:2965-73.

40. Macagno M, Bandini S, Stramucci L, Quaglino E, Conti L, Balmas E, et al. Multiple roles of perforin in hampering ERBB-2 (Her-2/neu) carcinogenesis in transgenic male mice. J Immunol 2014; 192:5434-41.

41. Bandini S, Curcio C, Macagno M, Quaglino E, Arigoni M, Lanzardo S, et al. Early onset and enhanced growth of autochthonous mammary carcinomas in C3-deficient Her2/neu transgenic mice. Oncoimmunology 2013; 2:e26137.

42. Conti L, De Palma R, Rolla S, Boselli D, Rodolico G, Kaur S, et al. Th17 cells in multiple sclerosis express higher levels of JAK2, which increases their surface expression of IFN-gammaR2. J Immunol 2012; 188:1011-8.

43. Regis G, Icardi L, Conti L, Chiarle R, Piva R, Giovarelli M, et al. IL-6, but not IFN-gamma, triggers apoptosis and inhibits in vivo growth of human malignant T cells on STAT3 silencing. Leukemia 2009; 23:2102-8.

44. McGinnes K, Chapman G, Marks R, Penny R. A fluorescence NK assay using flow cytometry. J Immunol Methods 1986; 86:7-15.

Table 1. NK cells in vitro killing without prior activation. TUBO, tumorsphere and yac-1 susceptibility to NK cells without any activation

	NK cell killing from BALB/C mice									NK cell killing from C57/BL6 mice								
	TUBO			Tumorspheres			Yac-1			TUBO			Tumorspheres			Yac-1		
E:T ratio	**12:1**	**6:1**	**3:1**	**12:1**	**6:1**	**3:1**	**12:1**	**6:1**	**3:1**	**12:1**	**6:1**	**3:1**	**12:1**	**6:1**	**3:1**	**12:1**	**6:1**	**3:1**
1° exp	15	3	0	38	25	10	65	46	22	15	10	7	45	24	18	60	36	12
2° exp	12	0	0	25	5	1	71	53	31	10	8	0	43	23	10	65	46	17
3° exp	2	0	0	15	7	0	59	41	20	5	0	0	21	5	0	51	32	5

Figure 1

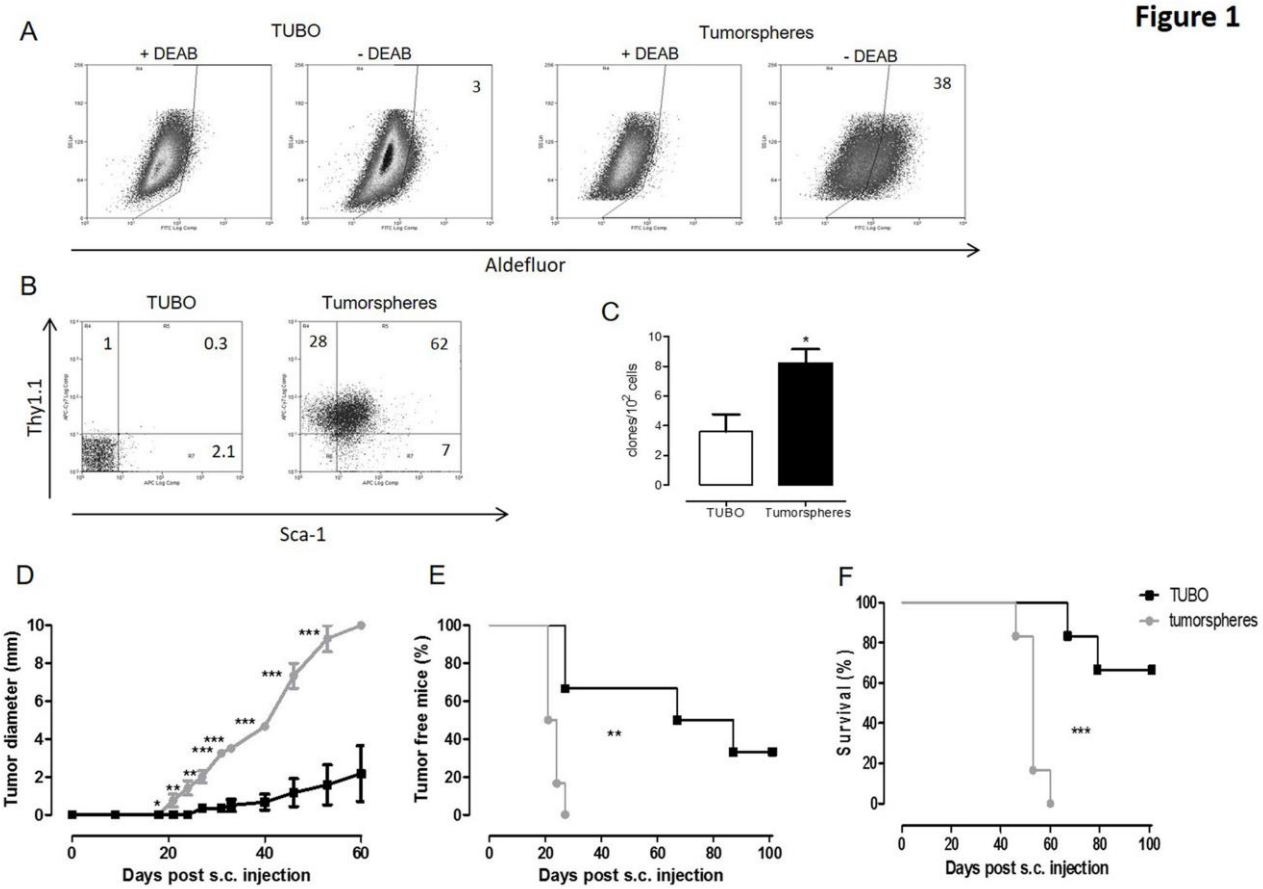

Figure 1

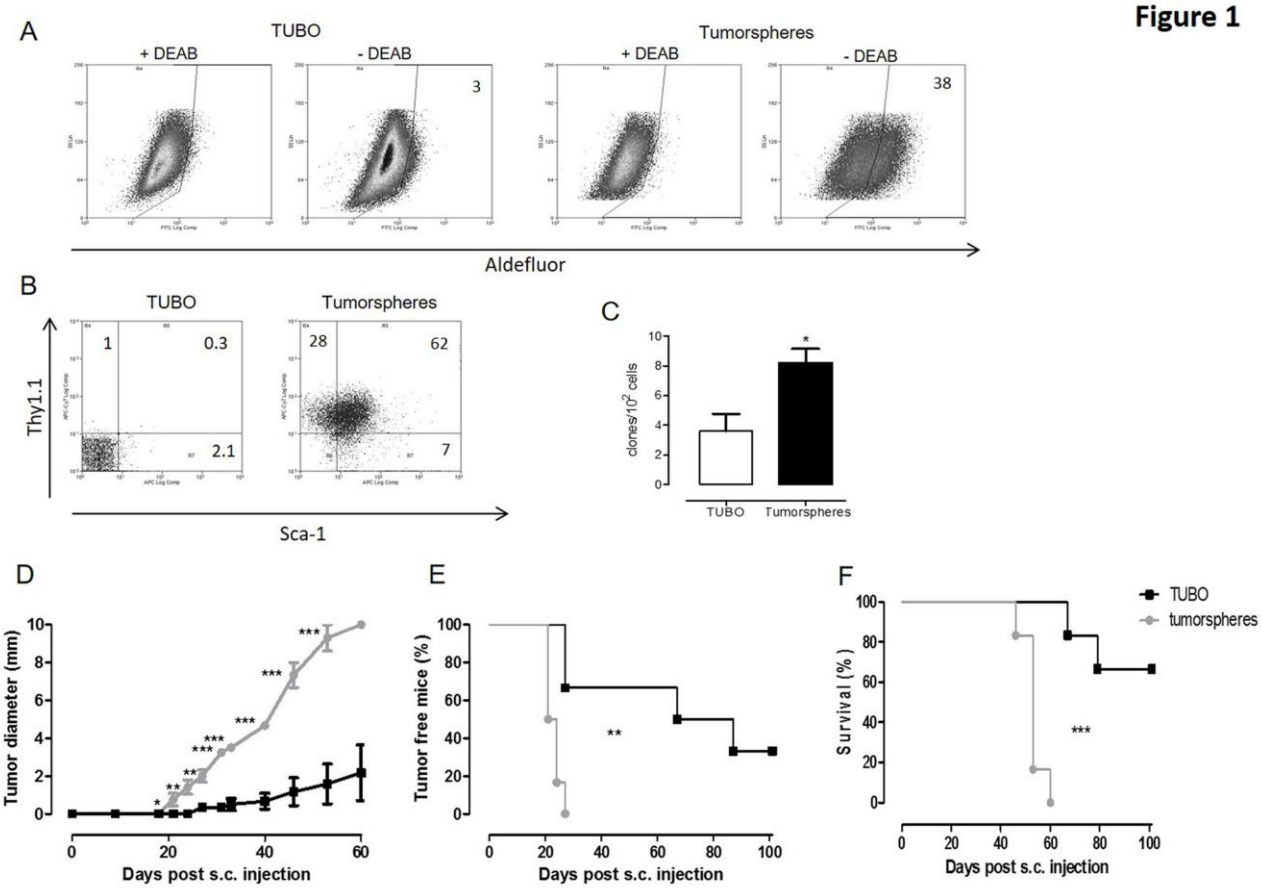

Figure 1. Tumorsphere characterization. (A) Representative FACS dot plots showing ALDH activity in TUBO and tumorspheres, measured using the Aldefluor reagent (right panels). To define the $ALDH^+$ gate, cells were stained with the Aldefluor reagent in the presence of the ALDH inhibitor DEAB (left panels). (B) Representative FACS dot plots showing the expression of Sca-1 and Thy1.1 in TUBO and tumorspheres. Numbers show the percentage of cells in each region. (C) Capability of TUBO and tumorspheres to give rise to cell clones in a limiting dilution assay. The graph shows the mean ± SEM of the number of clones generated every 10^2 single cells seeded; data are from three independent experiments. (D-F) Tumor growth (D), incidence (E) and Kaplan–Meier survival (F) curves of BALB/c mice s.c. injected with $1x10^3$ TUBO or tumorsphere-derived cells. Differences in mean tumor diameters were calculated using the Student's *t* test, while differences in tumor incidence and survival were performed using the Mantel-Cox log-rank test. * $p<0.05$; ** $p< 0.01$; *** $p \leq 0.001$.

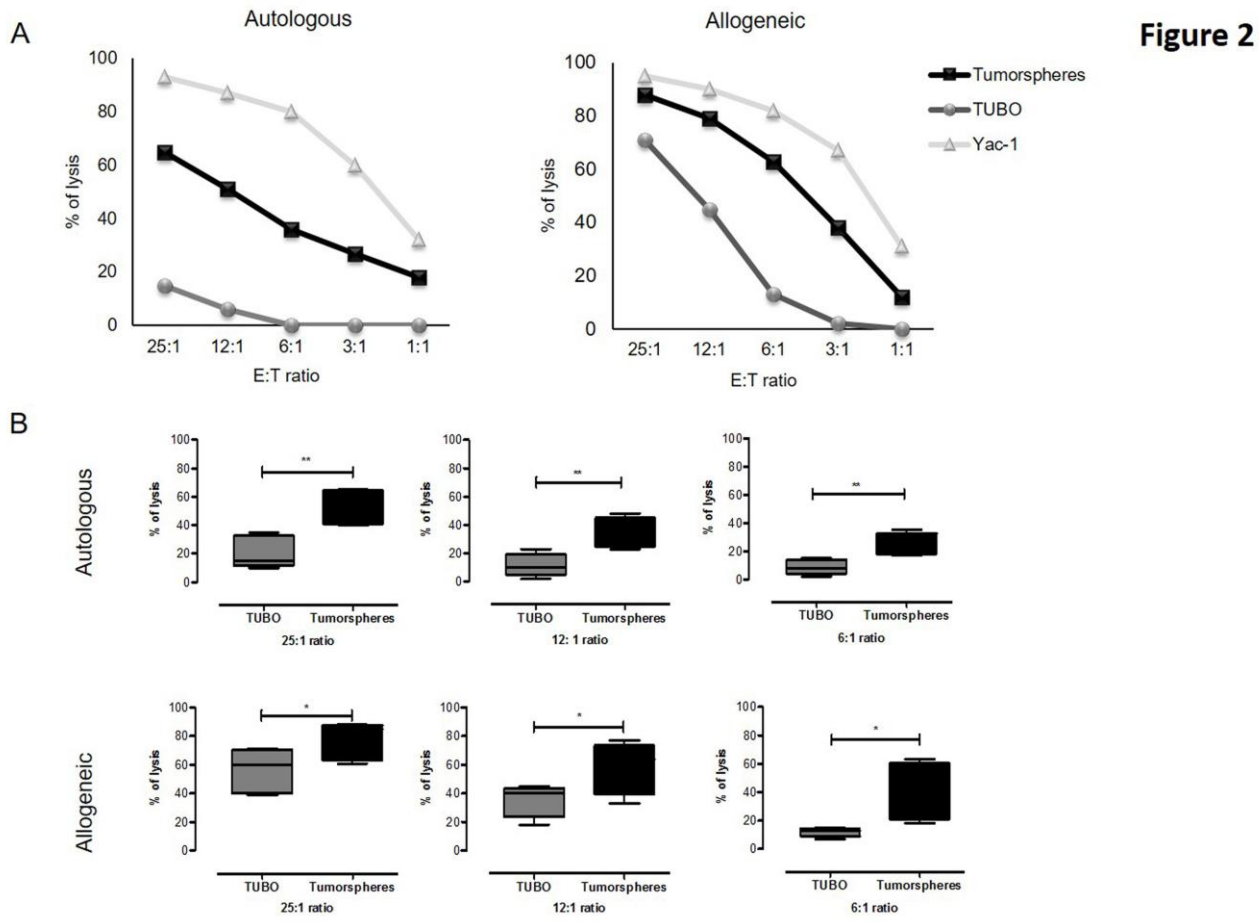

Figure 2. TUBO and tumorsphere susceptibility to NK cells. (A) A representative cytotoxicity assay, performed by culturing Yac-1 (triangle), TUBO cells (circles) and tumorspheres (squares) with autologous (from BALB/c, left panel) and allogeneic (from C57/BL6, right panel) splenocytes. NK cells were used at different E:T ratios, as reported on the X axes. (B) A statistical analysis of the data obtained from 5 independent cytotoxicity experiments at 3 different E:T ratios, with autologous NK cells (upper panel) and allogeneic NK cells (lower panel) against TUBO (grey bar) and tumorspheres (black bar). The mean ± SEM of the lysis (%) are reported. * $p \leq 0.05$; ** $p \leq 0.01$, Student's *t* test.

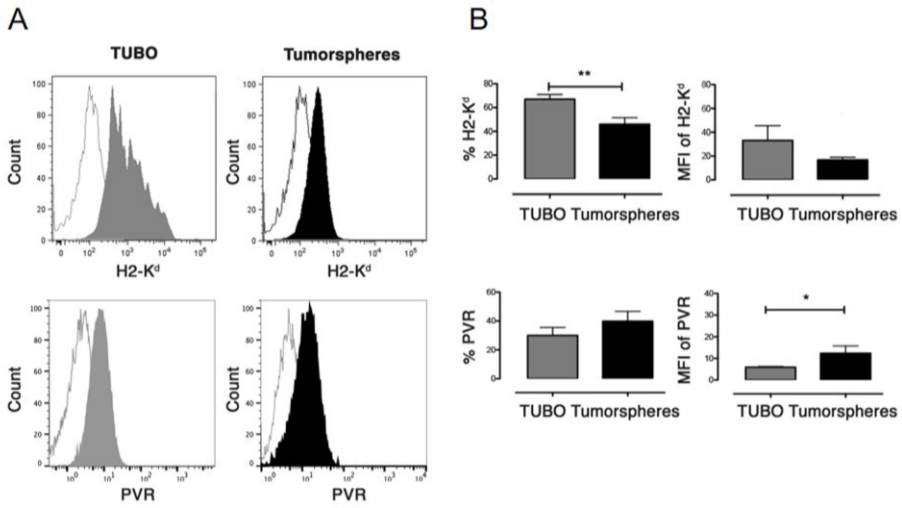

Figure 3. Phenotypic characterization of TUBO and tumorspheres. (A) A representative experiment showing the expression levels of the MHC class I (H2-K^d) and the PVR molecules on the cell surface of TUBO (grey) and tumorspheres (black). Filled histograms represent specific staining while open histograms represent the background of isotype controls. (B) Statistical analysis of the data obtained from 6 different experiments as a percentage of positive cells and mean fluorescence intensity (MFI) of H2-K^d and PVR on TUBO (grey bar) and tumorspheres (black bar). * $p \leq 0.05$; ** $p \leq 0.01$, Student's *t* test.

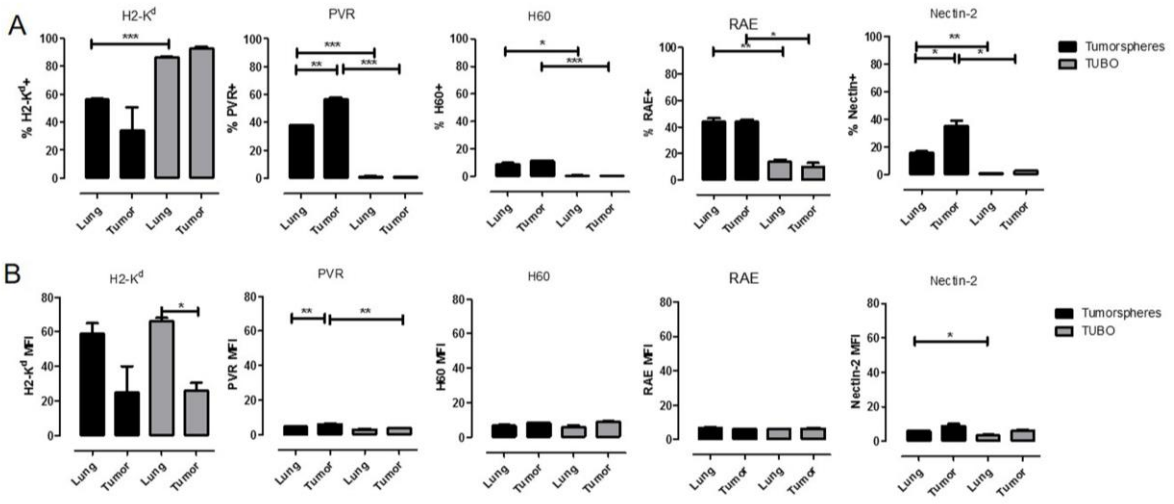

Figure 4. NK cell ligand expression on TUBO and tumorspheres *ex vivo*. Mean ± SEM of the percentage of positive cells (A) and of MFI (B) of H2-K^d, PVR, H60, Rae-1 and Nectin-2, on TUBO (grey bar) and tumorspheres (black bar) injected either s.c. (tumor) or i.v. (lung) into BALB/c mice, from three different experiments. * $p \leq 0.05$; ** $p \leq 0.01$, *** $p \leq 0.001$, Student's *t* test.

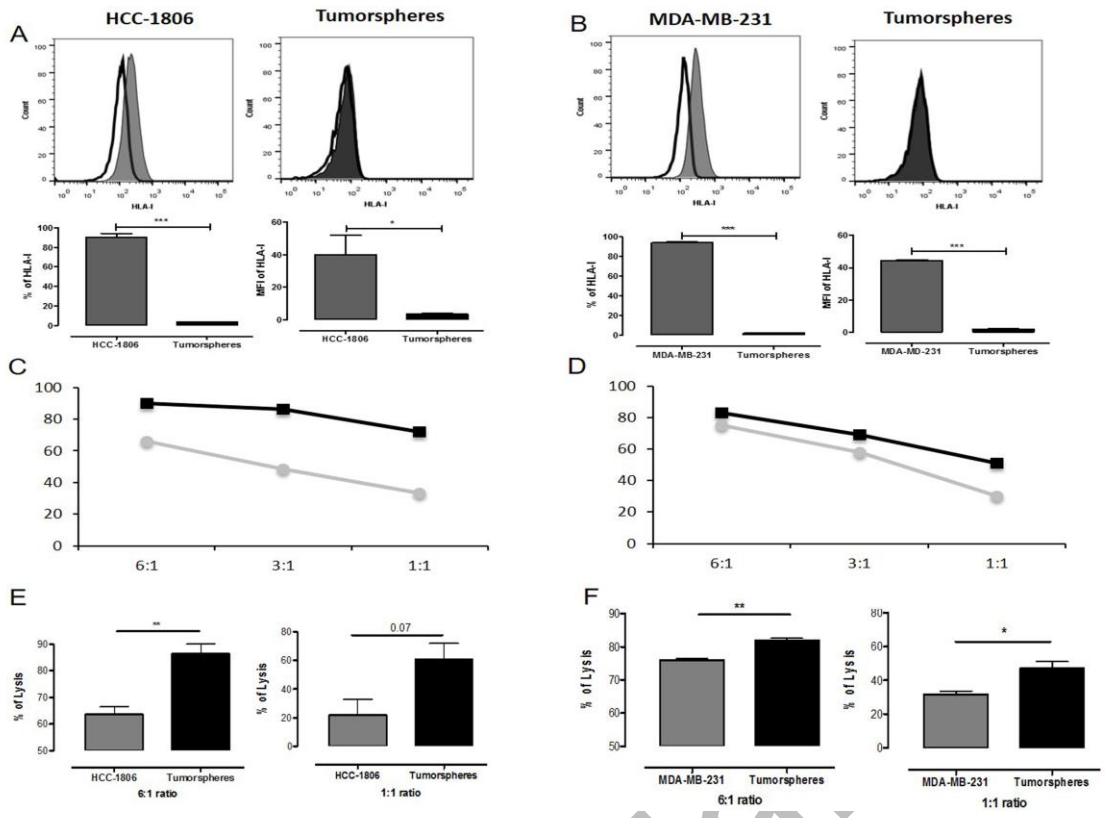

Figure 5. Phenotypic characterization and susceptibility to NK cells of HCC-1806 and MDA-MB-231 cells and their derived tumorspheres. (A, B) FACS analysis of the expression of the HLA-I molecules on HCC-1806 (A) and MDA-MB-231 (B) parental cells and tumorspheres. Filled histograms represent specific staining while open histograms represent the background of isotype controls. Graphs show the statistical analysis of the data obtained from 3 independent experiments as a percentage of positive cells and MFI of HLA-I on parental cells (grey bar) and tumorspheres (black bar). (C, D) A representative cytotoxicity assay performed by co-culturing HCC-1806 (C) and MDA-MB-231 (D) parental cells (circles) and tumorspheres (squares) with allogeneic lymphocytes. NK cells were used at different E:T ratios as reported on the X axes. (E, F) Means ± SEM of the percentage of lysis obtained from 3 independent cytotoxicity experiments at two different E:T ratios, with allogeneic NK cells against HCC-1806 (E) and MDA-MB-231 (F) parental cells (grey bar) and derived tumorspheres (black bar). * $p \leq 0.05$; ** $p \leq 0.01$, Student's *t* test.

Figure 6

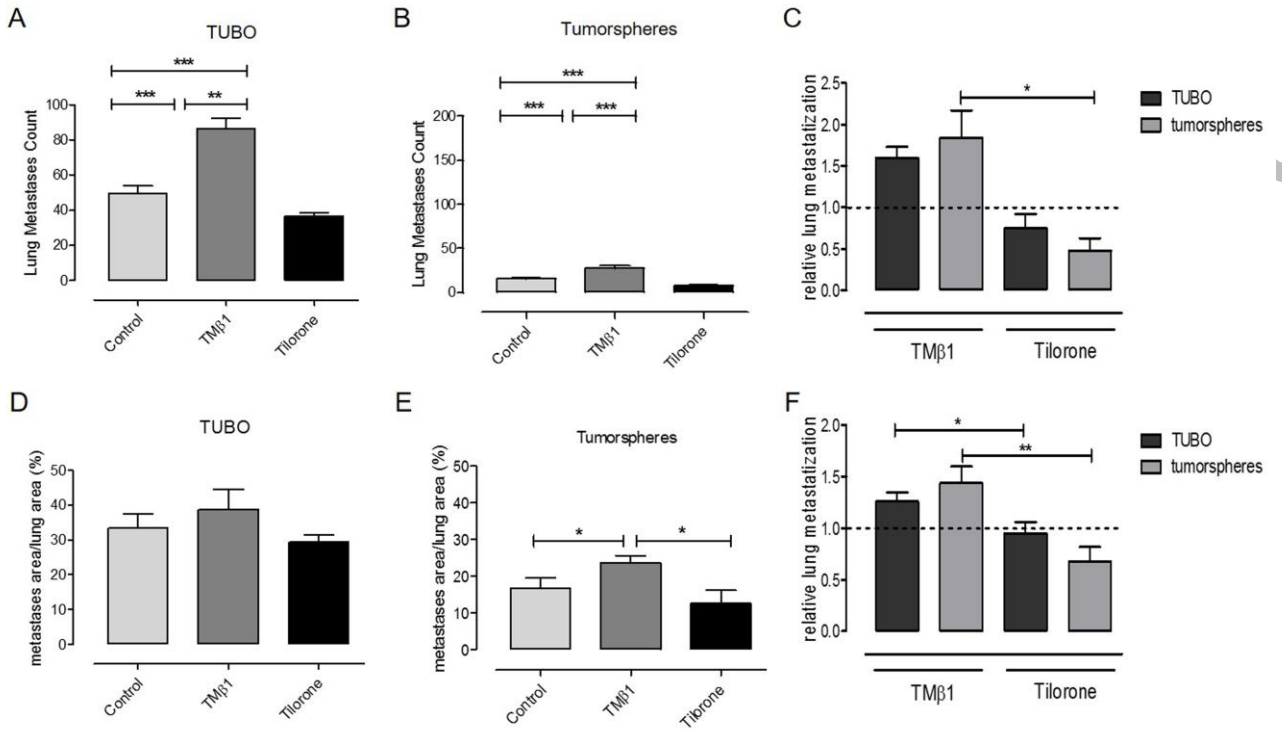

Figure 6. NK cells control lung metastasization. Number (A, B, C) and area (D, E, F) of lung metastases observed in BALB/c mice injected i.v. with either TUBO (A, D) or tumorspheres (B, E), and treated with either PBS (control), TMβ1 or tilorone. (C, F) Ratios between the number (C) and the area (F) of lung metastases of treated groups and their relative controls. Graphs show means ± SEM from 3 independent experiments. * $p \leq 0.1$, ** $p \leq 0.01$; *** $p \leq 0.001$, Student's *t* test.

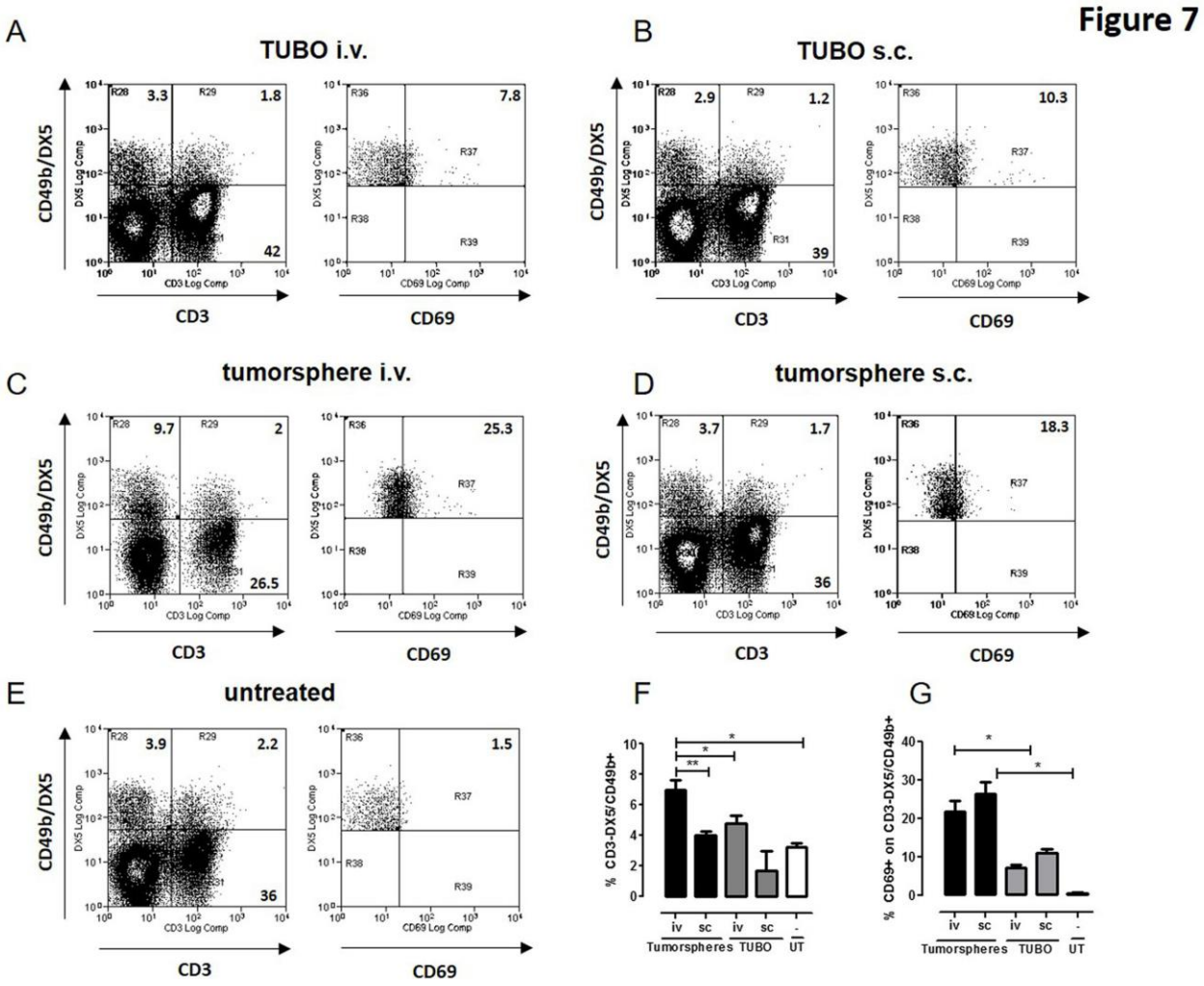

Figure 7. NK cell frequency in TUBO and tumorsphere challenged mice. FACS analysis of NK cells in the blood of BALB/c mice challenged either i.v. or s.c. with either TUBO (A,B) or tumorspheres (C,D) or left untreated (E), performed 21 days after i.v. cell challenge or when s.c. tumors measured 5 mm mean diameter. (A-E) Representative dot plots of the $CD3^{-}CD49b^{+}$ (left panels) and the $CD69^{+}CD3^{-}CD49b^{+}$ (right panels) populations. (F,G) Statistical analysis of the data cumulated from 3 independent experiments on the frequencies of NK cells in mice challenged either i.v. or s.c. with TUBO (grey bar) and tumorspheres (black bar) or left untreated (UT). * $p \leq 0.05$, ** $p \leq 0.01$; *** $p \leq 0.001$, Student's *t* test.

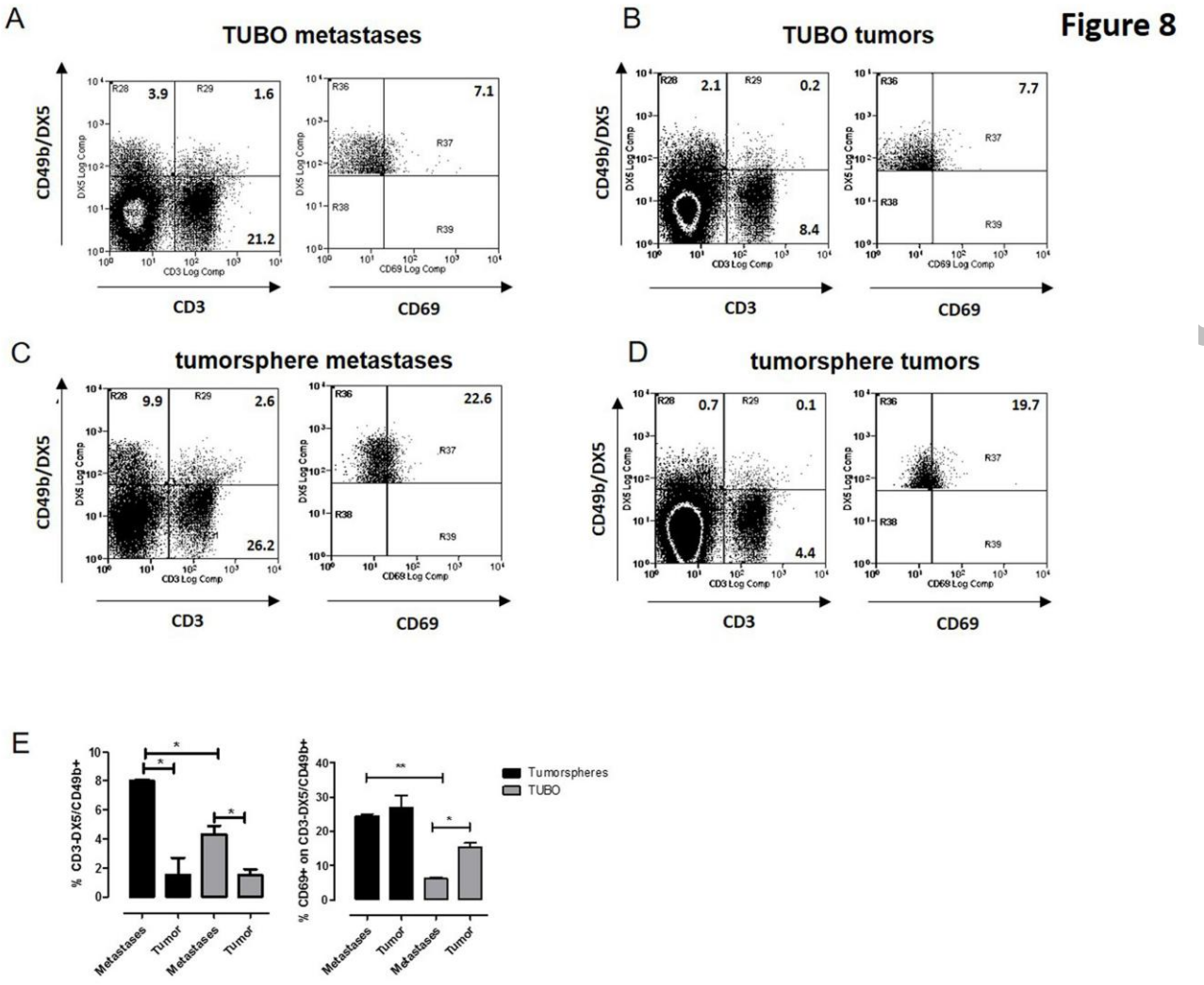

Figure 8. NK cell frequency in tumors and metastases of TUBO and tumorsphere challenged mice. FACS analysis of NK cells in TUBO (A,B), tumorspheres (C,D) metastases (A,C) and tumors (B,D) generated in BALB/c mice challenged either i.v. or s.c., performed 21 days after i.v. cell challenge or when s.c. tumors measured 5 mm in mean diameter. (A-D) Representative dot plots of the $CD3^{-}CD49b^{+}$ (left panels) and the $CD69^{+}CD3^{-}CD49b^{+}$ (right panels) populations. (E) Statistical analysis of the data cumulated from 3 independent experiments on the frequencies of NK cells in mice challenged either i.v. or s.c. with TUBO (grey bar) and tumorspheres (black bar). * $p \leq 0.05$, ** $p \leq 0.01$, Student's *t* test.